THE SEISMIC STRUCTURE OF THE SUN

D.O. Gough, A.G. Kosovichev, J. Toomre, E. Anderson, H.M. Antia, S. Basu, B. Chaboyer, S.M. Chitre, J. Christensen-Dalsgaard, W.A. Dziembowski, A. Eff-Darwich, J.R. Elliott, P.M. Giles, P.R. Goode, J.A. Guzik, J.W. Harvey, F. Hill, J.W. Leibacher, M.J.P.F.G. Monteiro, O. Richard, T. Sekii, H. Shibahashi, M. Takata, M.J. Thompson, S. Vauclair and S.V. Vorontsov

Abstract – GONG data reveal that the internal structure of the Sun can be well represented by a calibrated standard model. However, immediately beneath the convection zone and at the edge of the energy-generating core the sound-speed variation is somewhat smoother in the Sun than it is in the model. This could be a consequence of chemical inhomogeneity being too severe in the model, owing perhaps to inaccurate modelling of gravitational settling or to neglected macroscopic motion that may be present in the Sun. Accurate knowledge of the Sun's structure enables inferences to be made about the physics that controls the Sun, for example through the opacity, the equation of state or wave motion. Those inferences can then be used elsewhere in astrophysics.

[1]D.O. Gough, J.R. Elliott, T. Sekii: Institute of Astronomy, University of Cambridge; A.G. Kosovichev, P. Giles: HEPL, Stanford University; J. Toomre: JILA, University of Colorado; E. Anderson, J.W. Harvey, F. Hill, J.W. Leibacher: National Solar Observatory, Tucson; H.M. Antia, S.M. Chitre: Tata Institute for Fundamental Research, Bombay; S. Basu, J. Christensen-Dalsgaard: Theoretical Astrophysics Centre, Aarhus University; B. Chaboyer: Canadian Institute for Theoretical Astrophysics, Toronto; W.A. Dziembowski, Copernicus Astronomical Center, Warsaw; A. Eff-Darwich: Instituto Astrofisico de Canarias, Tenerife; P.R. Goode: New Jersey Institute of Technology, Newark; J. Guzik: Los Alamos National Laboratory, New Mexico; M.J.P.F.G. Monteiro: University of Oporto; O. Richard, S. Vauclair: Observatoire Midi-Pyrenees; H. Shibahashi, M. Takata: Department of Astronomy, University of Tokyo; M.J. Thompson, S.V. Vorontsov: Queen Mary and Westfield College, University of London.

One of the principal purposes of the GONG project is to determine the internal structure of the Sun. Helioseismology is used to model the stratification of density ρ, the internal stress that supports the star, and the relation between them when they are adiabatically perturbed *(1)*. In the absence of a magnetic field or small-scale turbulence, the stress is the gradient of the pressure p. Then perturbations of ρ and p are related via the adiabatic exponent γ_1 *(2)*. The variation of these quantities with position is determined by seismology, and constitutes what we call the seismic structure of the Sun. One must use properties of theoretical solar models for inferring other quantities such as temperature (2). Theoretical models also provide a reference against which to compare the seismic model.

The traditional manner of inferring the structure of the Sun is to calibrate a theoretical model: that is to say, to adjust a set of uncertain parameters which specify the model until a best fit with the data is obtained. Difficulty arises when the model cannot be adjusted to fit all the data within the estimated measurement errors, indicating a fundamental error in the model. Various techniques, known as inverse methods, consider a wider class of possible structures by relaxing some of the basic assumptions upon which the theoretical models are based *(3)*. By so doing, one can come closer to explaining what the data might imply, and hence obtain a representation of the Sun that is in better accord with those data.

Many inverse methods seek differences between certain aspects of the Sun and a theoretical model. If the structure of the model is close to that of the Sun, the equations relating the two can be simplified by linearization. By a sequence of refinements it has been possible to produce a model which in many respects is very close to the Sun *(4)*. That model now serves both as a reference with which to compare the Sun, and as a guide to interpreting the differences we find.

Analyzing the frequencies of modes of oscillation is one means whereby the structure of the Sun can be inferred. One can also study the shapes of the oscillating disturbances

– the so-called eigenfunctions – or one can investigate over a limited region of the Sun the propagation of the component waves which constitute those eigenfunctions *(5)*. Such studies are best suited to the investigation of lateral inhomogeneity. Nevertheless, most of the inferences to date have been obtained from global mode frequencies, and it is accordingly to these that we restrict attention in this article.

Seismic waves

Acoustic seismic waves propagate through the solar interior along ray paths almost in planes through the center of the Sun (Fig. 1). After reflection at the surface, the waves propagate downwards, to be refracted by the sound-speed gradient back to the surface where they are reflected again. Notice that the paths are not closed, so that after many reflections the waves sample essentially the entire region outside a central zone of avoidance, and therefore provide a global diagnostic of that region. Indeed, if there were no attenuation by dissipation, a single ray would fill the accessible space. The waves of particular interest are those whose frequencies are such that on neighboring paths the waves are essentially in phase. This leads to constructive interference, and the formation of a resonant mode of oscillation with a well defined frequency *(6)*.

For a wave to be observed, the disturbance must pass from the interior of the Sun to the photosphere through the ill-understood surface layers which influence the oscillation frequencies in a significant but partly unknown way. That influence must be eliminated from the data.

The detailed geometry of the ray paths, and consequently the values of the resonant frequencies, are determined principally by the variation of the sound speed c through the Sun *(7)*. Broadly speaking, the extent to which any given region of the Sun influences the resonant frequency is proportional to the time spent in that region by an imaginary point traveling with the wave *(8)*. This is represented in Figs. 1A and 1B by the intensity of the brown and red shading. The shading is dense near the surface of the star, where the wave speed is low. It is also relatively dense near the edge of the zone of avoidance, for

although the wave speed is relatively high, the ray density is large: the imaginary point passes through the region many times. Indeed, the ray density is formally infinite at the boundary of the zone of avoidance, to which the rays are tangent. This boundary is called a caustic.

The difference between a measured oscillation frequency of the Sun and that of a corresponding mode of a theoretical model can be represented as an average of the difference between the solar and the model wave speeds *(9)*. However, the implications of such averages are not easy to comprehend, because they are made up of contributions from many parts of the Sun. What we would prefer is to be told the actual sound-speed difference δc at each point, but that is not possible. What is possible, however, is to be given a sequence of averages each of which is localized in space. To understand how such an average is obtained, consider the difference between the frequencies of the modes in Fig. 1A and 1B: that provides an average of the sound-speed difference weighted with the difference between the corresponding weight functions (Fig. 1C). The new weight function is greatest in the vicinity of the caustics, there having been substantial cancellation elsewhere. Thus the frequency difference provides localized information about the sound speed. A sequence of such averages can be thought of as a blurred representation of the function δc. More highly localized averages can be obtained by taking appropriate combinations of a greater number of frequencies. With enough modes one can eliminate the contribution from the surface, whereas in Fig. 1C cancellation was far from complete. Some examples of well localized weight functions are displayed in Fig. 2A.

One can instead represent the sound-speed difference in terms of a predetermined set of functions, choosing the linear combination that best fits the data. Since emphasis here is on reproducing the data, the method is akin to the calibration of solar models, except that here the representation is not constrained to satisfy the equations that govern those models. Moreover, the number of adjustable parameters is typically much greater. Interestingly, when one has a wide range of modes such as those in the GONG dataset,

the value of the resulting function at any point is an average of the actual sound-speed difference which is usually localized in the vicinity of that point *(10)*.

A third technique has the advantage of not relying on a reference model (Fig. 2B). If the structure of the Sun were known above the caustic of the shallower mode, the frequency of that mode could be calculated. The structure of the more deeply penetrating wave could be calculated above the caustic of the shallower mode, and its frequency would then be calculable in terms of the unknown sound speed in the thin region between the two caustics. A measurement of the frequency would therefore determine the sound speed averaged over this thin region. From the frequencies of a succession of modes that penetrate more and more deeply, it is evident that in principle one can build up a picture of the sound-speed variation *(11)*.

Inferences from GONG data

In Fig. 3 we plot the square of the sound speed in the Sun, obtained from GONG data, and also that in a reference model *(12)*. The agreement is close. Only near the base of the convection zone and in the energy-generating core are there discrepancies. The former is evident in the enlargement of the vicinity of the base of the convection zone (inset Fig. 3).

The adiabatic stratification in the Sun appears to penetrate about $0.002R$ more deeply than in the model *(13)* (here R is the radius of the Sun). Also, the values of $u = p/\rho$, and consequently c^2 (2), converge quickly at greater depths (Fig. 4). Part of the difference in u between Sun and model could be associated simply with the fact that the model convection zone may be too shallow. However, the excess u caused by that property is of lesser magnitude than that in the figure, and extends more deeply (3). The small positive value of $\delta u/u$ between $0.3R$ and $0.6R$ might therefore be accounted for in this way, but the relatively sharp bump between $0.6R$ and $0.7R$ cannot. The decrease in u locally may indicate that immediately beneath the convection zone the accumulation of helium, which augments the mean molecular mass μ (2), has been overestimated in the reference model.

This is consistent with recent computations *(14–17)*, some results of which are compared with the Sun in Fig. 5. The bump could in principle have been produced by an opacity error that drops abruptly to zero immediately beneath the base of the convection zone. However, such a fortuitous occurrence is unlikely.

The discrepancy in the core is the third prominent feature. Most secure is the negative region of $\delta u/u$ between about $0.1R$ and $0.2R$, which implies that the variation of u itself is flatter than in the model (cf Fig. 3). Once again this would be a symptom of there being too steep a composition gradient in the model, which here has been produced by nuclear reactions. The density inversion (Fig. 4) is consistent with this interpretation: the regions of relatively steep positive slope in $\delta\rho/\rho$ in the core and immediately beneath the convection zone imply that the magnitude of the (negative) gradient of density is too high in the model *(18)*.

A certain amount of turbulent mixing reduces the discrepancy immediately beneath the convection zone (Fig. 5A,B). We have constructed models with somewhat different helium redistribution which reduce the discrepancy further, yet that does not imply that mixing is necessarily the solution. A model which also well represents the Sun near the base of the convection zone (Fig. 5C) has no such mixing, but instead suffers mass loss during the course of its evolution. The upward flow of material into the convection zone, and subsequently out into the solar wind, counteracts the settling of helium, leaving a smaller helium concentration between $0.6R$ and $0.7R$. We estimate the helium abundance to be 0.248 ± 0.005 in the convection zone where the stratification is adiabatic. This value is similar to previous estimates *(19)*.

Deviations from spherical symmetry split the degeneracy of the mode frequencies with respect to m. The component of the splitting that is odd in m is produced by those aspects of rotation that depend on odd powers of the angular velocity Ω, the even component by everything else (including phenomena such as centrifugal force which depend on even powers of Ω, and which cannot distinguish east from west). Here we consider only the

even splitting, leaving discussion of rotation to *(20)*.

We determine the component of the deviation from spherical symmetry that is axisymmetric about the rotation axis. Only processes that produce a deviation in the wave propagation speed, or a distortion to the shape of the cavity within which the waves propagate, influence the frequencies of the modes. Wave speed can be modified by sound-speed deviations and by a magnetic field, or the wave can be advected by the component of large-scale material flow in meridional planes *(21)*. Unfortunately one cannot distinguish between them by seismic frequency analysis alone *(22)*. Therefore we simply express the outcome of our analysis as a scalar wave-speed variation. Inversions are carried out in a manner analogous to those for the spherically averaged structure, except that now the latitudinal dependence of the waves must be taken into account *(23)*.

The only significant aspherical variation is confined to a shallow layer immediately beneath the solar surface (Fig. 6). This finding is consistent with previous inferences *(24)*. Moreover, the variation of wave speed with latitude is very similar to the brightness temperature of the solar atmosphere, which confirms previous findings *(24)*. The wave-speed variation (Fig. 7) is less well resolved than the spherically averaged sound speed (Figs. 3–5), and is therefore less reliable. The reason is that it depends on very small frequency differences, which are of order 0.1μHz, rather than on the full mode frequencies. As GONG runs for longer, the results will improve. However, the precision will be limited by the structural changes that the Sun will undergo in the course of the solar cycle.

There is no significant asphericity (Figs. 6 and 7) beneath $r \simeq 0.9R$. Therefore, we find no evidence for a deeply seated thermal perturbation or magnetic field. If there were a field concentrated in a layer of thickness $0.1R$, say, as some dynamo theorists have postulated *(25)*, we could set an upper bound to its average intensity over that layer of a few tens Tessla. That bound is not inconsistent with dynamo models *(25)*.

We have made two suggestions that might possibly account for the discrepancies in the sound speed: mass loss and material mixing. Both require that material now in the

convection zone has previously been at higher temperature. That could have caused the light chemical elements lithium and beryllium to have been partially destroyed by nuclear reactions. Both possibilities have been proposed before to explain the observed Li and Be deficiencies in the atmospheres of the Sun and other similar stars; now we have evidence that one of them might be correct. The model in Fig. 5C has lost 10% of its mass, most of it in the first 10^9 years., and it reproduces the observed lithium deficiency in the solar photosphere. However, there are also plausible mechanisms for material mixing, including weak convective overshooting *(26)*, nonlinear wave transport *(27)*, rotationally induced shear turbulence *(28)* and Ekman circulation *(29)*. To distinguish the different possibilities will require a more highly resolved picture of the transition at the base of the convection zone *(30)*, including the shear in the angular velocity *(20)*.

The discrepancy in the energy-generating core might also be a symptom of macroscopic motion, which transports the products of the nuclear reactions from their sites of production. That would modify the neutrino emission rates, and thereby change the status of the solar neutrino problem, despite evidence that at least part of the problem lies in elementary-particle physics *(32)*. It would also lengthen the life expectancy of the Sun, by replenishing spent hydrogen fuel. The implications are far reaching: for example, if other stars behave similarly, the conflict between the age estimates of globular clusters and some lesser age estimates of the Universe would be exacerbated. Such motion would also transport angular momentum. It would therefore leave a signature in the variation of angular velocity in the core.

References and notes

1. Except in the very surface layers of the Sun, the characteristic cooling time is much longer than the periods of the seismic waves, so the wave motion is essentially adiabatic. Near the surface the Sun is highly turbulent, and is not well understood.

2. The adiabatic exponent γ_1 is the thermodynamic quantity $(\partial \ln p/\partial \ln \rho)_s$, the partial derivative being taken at constant specific entropy s. It determines the so-called sound speed c according to $c^2 = \gamma_1 u$, where $u = p/\rho$. For a perfect gas, which provides a guide to the equation of state of solar material, $u = T/\mu$, where μ is the mean 'molecular' mass of the material (i.e. mean mass per particle - atom or ion - measured in atomic units). Since chemical composition, and therefore μ, are not well determined in the Sun, to infer T one must consider the balance of thermal energy production against energy transport, neither of which are reliably understood, particularly the latter. In Figs. 4 and 5 we display relative differences in u; except in the ionization zones of hydrogen and helium near the surface of the Sun ($r \gtrsim 0.95R$), $\gamma_1 \simeq 5/3$, and $\delta u/u \simeq \delta c^2/c^2$.

3. D.O. Gough, *Solar Phys.* **100**, 65 (1985); A.G. Kosovichev, *Bull. Crimean Astrophys. Obs.* **75**, 36 (1986); D.O. Gough, and A.G. Kosovichev, *Inside the Sun* (Proc. IAU Colloq. 121, G. Berthomieu and M. Cribier, eds. Kluwer, Dordrecht) p.327 (1990); D.O. Gough and M.J. Thompson, *Solar interior and atmosphere.* (A.N. Cox, W.C. Livingston and M. Matthews, eds. Tucson, AZ, University of Arizona Press), 519 (1991); W.A.Dziembowski, A.A. Pamjatnykh and R. Sienkiewicz, *Mon. Not. Roy. astron. Soc.* **249**, 602, (1991).

4. J. Christensen-Dalsgaard and W. Däppen *et al.*, 1996, *Science*, this issue

5. J. Patron, F. Hill, E.J. Rhodes, Jr., S.G. Korzennik and A. Cacciani, *Astrophys. J.* **455**, 746 (1995); T.L. Duvall, Jr., S. D'Silva, S.M. Jefferies, J.W. Harvey and J. Schou, *Nature* **379**, 235 (1996); A.G. Kosovichev, *Astrophys. J. Lett.* **461**, L55 (1996).

6. J.B. Keller and S.I. Rubinow, *Ann. Phys.* **9**, 24 (1960); D.O. Gough, *Astrophysical Fluid Dynamics.* (J.P. Zahn and J. Zinn-Justin, eds. North-Holland, Amsterdam), 399 (1993). In a sphere, like the Sun, the phases of waves on adjacent planes containing the center of the sphere must also be in appropriate relative phase for resonance to occur.

7. Frequencies depend also on the variation of density, but to a lesser extent than they do on sound speed (see note 9).

8. That time is inversely proportional to the magnitude of the group velocity and is directly proportional to the relative density of ray-path segments.

9. Because resonance results from constructive phase coherence, it is the phase speed that is relevant here. In a uniform fluid, the group and phase speeds have the same value, c, which satisfies $c^2 = \gamma_1 p/\rho$. But in a medium stratified under gravity, like the Sun, density gradients cause the two speeds to differ. A magnetic field would also contribute to the difference. Here the term 'wave speed' always means phase speed, which is higher than the magnitude of the group velocity. Except near the surface of the Sun, both the phase and the group speeds are almost the same, and accordingly in the text we shall often use the term 'sound speed' to denote phase speed, because it is more familiar. When comparing the Sun with models we use c^2 or $u = p/\rho$ rather than c because, being proportional to T/μ, it is more readily comprehended.

10. J. Christensen-Dalsgaard, J. Schou, and M.J. Thompson, *Mon. Not. Roy. Astron. Soc.* **242**, 353 (1990).

11. This technique has been carried out only using asymptotic representations of the resonance conditions, e.g. J. Christensen-Dalsgaard *et al., Nature* **315**, 378 (1985).

12. As discussed earlier in the text, what the seismic data give us are averages of the structure variables. The difference $\delta\nu_i$ between the frequencies of a mode (labeled i) of the Sun and of the reference model can be written $\delta\nu_i = \int K^i_{c^2,\gamma_1}\, \delta \ln c^2 \, \mathrm{d}r +$

$\int K^i_{\gamma_1,c^2}\delta\ln\gamma_1\ \mathrm{d}r$. The data kernels $K^i_{c^2,\gamma_1}$ and $K^i_{\gamma_1,c^2}$ are functions of the eigenfunctions of oscillation, and examples of the former are represented in brown and red in Fig. 1. Localized averages of the relative differences in c^2 are obtained from $\int \mathcal{K}_{c^2,\gamma_1}\delta\ln c^2\ \mathrm{d}r = \Sigma\alpha_i\delta\nu_i - \int \mathcal{K}_{\gamma_1,c^2},\delta\ln\gamma_1\mathrm{d}r$ by neglecting the second term on the right-hand side, where the averaging kernel $\mathcal{K}_{c^2,\gamma_1}(r;r_0) = \Sigma\alpha_i(r_0)K^i_{c^2,\gamma_1}$ is concentrated near $r = r_0$ and $\mathcal{K}_{c^2,\gamma_1} = \Sigma\alpha_i K^i_{\gamma_1,c^2}$ is everywhere small. References 3 explain how the coefficients α_i are computed. Examples of averaging kernels are displayed in Fig. 2A. The subsidiary variable to c^2, here γ_1, could be any function of the seismic structure that is independent of c^2, such as ρ. We have carried out inversions for several different pairs of variables, to confirm the robustness of our inferences against contamination by the neglected integral of the second variable. The averaging kernels can be dangerously large very near the surface, where all the data kernels are large, particularly when least-squares frequency-fitting techniques are used to construct α_i. Indeed, it is partly for this reason that naive fitting of raw frequencies can be misleading. To obviate contamination by surface effects one subtracts from all $\delta\nu_i$ an arbitrary function of ν_i divided by the modal inertia, which is the functional form of any surface uncertainty (see ref. 3).

13. That sets the radius of the base of the adiabatically stratified part of the convection zone at about $0.709R$. This value is somewhat less than the value $0.713R$ obtained previously by J. Christensen-Dalsgaard, D.O. Gough and M.J. Thompson, *Astrophys. J.* **378**, 413 (1991), and by A.G. Kosovichev and A.V. Fedorova, *Sov. Astron.* **35**, 507 (1991). A study of the transition at the base of the convection zone (see note 30) is consistent with the new result, although a repeat of the analysis using reference models of Richard *et al. (15)* yields $0.714R$.
14. S. Basu and H.M. Antia, *Mon. Not. Roy. Astron. Soc.* **269**, 1137 (1995).
15. O. Richard *et al., Astron. Astrophys.*, in press.
16. B. Chaboyer, P. Demarque and H.M. Pinsonneault, *Astrophys. J.* **441**, 865 (1995).

17. J.A. Guzik, A.N Cox, *Astrophys. J.* **448**, 905 (1995).

18. In the cores of solar models the values of p and T are more robust than ρ and μ: the reason is that pressure supports the weight of the star, which is determined principally by the mass which is a known quantity, and the nuclear reaction rates, which are observationally constrained by the Sun's radiative luminosity, are sensitive to T. Therefore, since $\gamma_1 \simeq 5/3$ in the essentially fully ionized core, $\delta \ln c^2 \propto -\delta \ln \rho \propto -\delta \ln \mu$: a local increase in c^2 tends to be associated with corresponding relative decreases in ρ and μ.

19. W.A. Dziembowski, A.A. Pamjatnykh and R. Sienkiewicz, *Mon. Not. Roy. Astron. Soc.* **249**, 602 (1991); W. Däppen *et al., Challenges to theories of the structure of moderate-mass stars*, (D.O. Gough and J. Toomre, eds. Springer, Heidelberg), *Lecture Notes in Physics* **388**, 111 (1991); A.G. Kosovichev *et al., Mon. Not. Roy. astron. Soc.* **259**, 536 (1992); H.M. Antia, S. and Basu, *Astrophys. J.* **426**, 801 (1994); A.G. Kosovichev, *Element Abundance Variations in the Sun and Heliosphere.* (The Thirtieth COSPAR Scientific Assembly, Hamburg, Germany) *Advances in Space Res.* **15**, no.7, p. 95 (1995).

20. M.J. Thompson and J. Toomre, *et al.*, 1996, *Science*, this issue

21. The wave is also advected by azimuthal flow, but the axisymmetric component of that is rotation, which is addressed in *(20)*.

22. E.G. Zweibel and D.O Gough, in *Proc. Fourth SOHO Workshop: Helioseismology* (J.T. Hoeksema *et al.*, eds., ESA SP-379, Noordwijk) **2**, 37 (1995). Although one cannot distiguish between possible sources of asphericity by analyzing frequencies alone, the different anisotropies of the wave-speed perturbations from different sources renders it possible in principle to distinguish them by their eigenfunctions. That might become reality in future, using techniques such as time-distance seismology.

23. The averaging kernels in this case are quadratic in the horizontal structure of

the eigenfunctions. They are therefore even functions of latitude, and are sensitive only to the north-south symmetric component of the asphericity. It requires some knowledge of the form of the eigenfunctions to determine the asymmetric component.

24. D.O. Gough and M.J. Thompson, *Advances in helio– and asteroseismology*, J. Christensen-Dalsgaard and S. Frandsen, Eds. (Reidel, Dordrecht, 1988), pp. 175–180; J.R. Kuhn, *Astrophys. J. Lett.* **331**, L131 (1988); P.R. Goode and J.R. Kuhn, *Astrophys. J.* **356**, 310 (1990); K.G. Libbrecht and M.F. Woodard, *Astrophys. J.* **402**, L77 (1993).

25. E.A. Spiegel and N.O. Weiss, *Nature* **287**, 616 (1980); C.A. Morrow, P.A. Gilman and E.E. DeLuca, in *Seismology of the Sun and Sun-like stars* (ed V.Domingo and E.J. Rolfe, ESA SP-286, Noordwijk), p.109 (1988); S. Moreno-Insertis, in *Sunspots: Theory and Observation*, (ed. J.H. Thomas and N.O. Weiss, Kluwer, Dordrecht).

26. D.O. Gough and T. Sekii, *Astron. Soc. Pac. Conf. Ser.* **42**, 177 (1993); M.J.P.F.G. Monteiro, J. Christensen-Dalsgaard and M.J. Thompson, *ibid*, p.253; A.G. Kosovichev, *Advances in Solar Physics*, (G. Belvedere, M. Rodono and G.M. Simnett, eds. Proc. of the Seventh European Meeting on Solar Physics, Springer-Verlag), *Lecture Notes in Physics* **432**, 47 (1994); S. Basu and H.M. Antia, *Mon. Not. Roy. Astron. Soc.* **269**, 1137 (1995).

27. D.O. Gough, *Solar-terrestrial relationships and the Earth environment in the last millenia*, (G. Castagnoli-Cini, ed., *Italiana Fisica*, Bologna), p.90 (1988); E. Knobloch and W.J. Merryfield, *Astrophys. J.* **401**, 196 (1992).

28. J.-P.Zahn, *Astron. Astrophys.* **265**, 115 (1992)

29. E.A. Spiegel and J.-P. Zahn, *Astron. Astrophys.* **265**, 106 (1992)

30. We have investigated the structure of the transition between the convection zone and the radiative interior by first considering how mode frequency varies with the phase difference between the surface of the Sun and the base of the convection zone,

after having filtered out surface effects, and then comparing it with theoretical models *(31)*. The signature of the transition oscillates with phase, in step with the eigenfunctions, with an amplitude which is smaller than that of the reference model, confirming that, if spherical, the transition is smoother than that of the model. The apparent smoothness might have come about because what has been observed is actually the spherical average of an aspherical structure. We note that adiabatic convective overshooting is likely to increase the amplitude; therefore if such overshooting occurs in the Sun the physical discrepancy is actually greater than it appears at first sight. There is some indication that the amplitude of the oscillatory signal varies with the ratio m/l of azimuthal order to degree. This suggests that the structure of the lower boundary layer of the convection zone might vary with latitude. Although at present this is no more than a hint, it points to an exciting direction of research with further long-term seismic data.

31. M.J.P.F.G. Monteiro and M.J. Thompson, *Astron. Astrophys.* **283**, 247 (1994), J. Christensen-Dalsgaard, M.J.P.F.G. Monteiro and M.J. Thompson, *Mon. Not. Roy. Astron. Soc.* **276**, 283 (1995); I.W. Roxburgh and S.V. Vorontsov, *ibid.* **268**, 880 (1994); S. Basu, H.M. Antia and D. Narasimha, *ibid.* **267**, 207 (1994).

32. J.N. Bahcall and H.A. Bethe, *Phys. Rev.* **D47**, 1298 (1993)

33. This work utilizes data obtained by the Global Oscillation Network Group (GONG) project, managed by the National Solar Observatory, a Division of the National Optical Astronomy Observatories, which is operated by AURA, Inc. under a cooperative agreement with the National Science Foundation. The data were acquired by instruments operated by the Big Bear Solar Observatory, High Altitude Observatory, Learmonth Solar Observatory, Udaipur Solar Observatory, Instituto de Astrofísico de Canarias, and Cerro Tololo Interamerican Observatory. We acknowledge financial support from the UK Particle Physics and Astronomy Research Council, the National Science Foundation, the National Aeronautics and Space

Administration and Danmarks Grundforskningsfond.

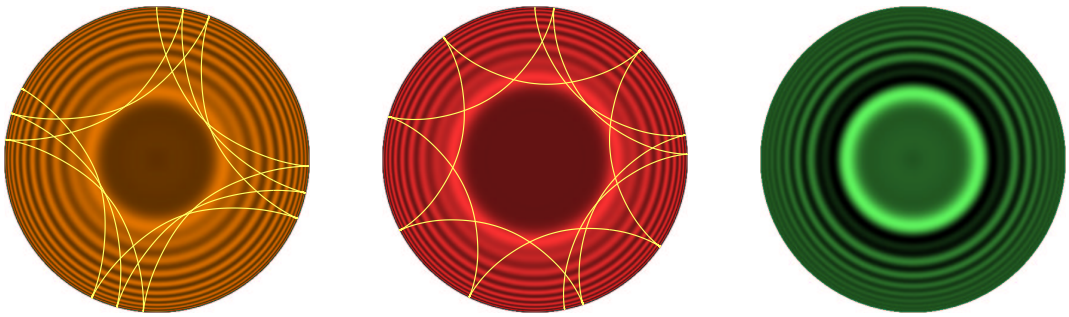

Figure 1: The first two images depict acoustic ray paths for modes with $n = 20$, $l = 1$ and $n = 20$, $l = 2$, which have similar frequencies, but penetrate to different depths. The extent to which the structure of the Sun influences their frequencies is represented by the intensity of the brown and red shading. The third image is the result of subtracting the red from the brown, the green intensity representing the sensitivity to the frequency difference. Notice that the greatest intensity is in the region between the lower limits (caustics) the two ray paths in A and B.

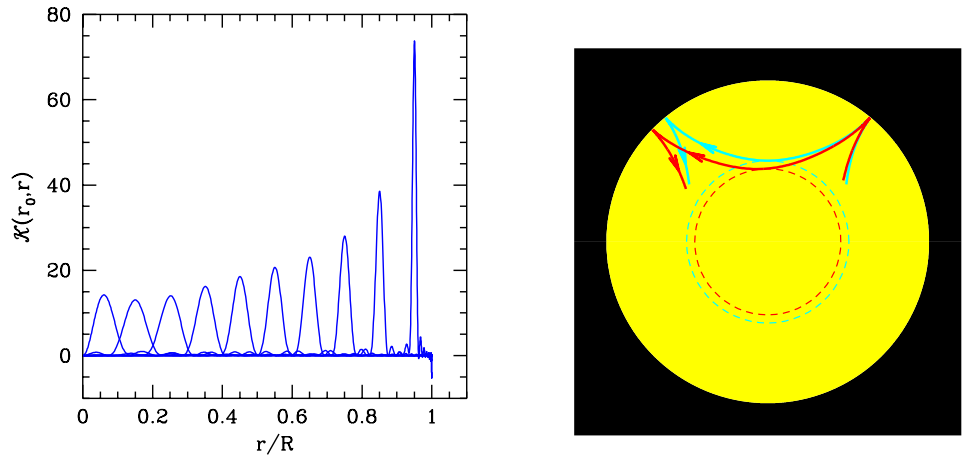

Figure 2: A Localized averaging kernels, which weight averages of sound-speed differences between the Sun and a theoretical reference model. B Portions of the ray paths depicted in Figs. 1 A (blue) and B (red). The dotted circles are the corresponding caustics.

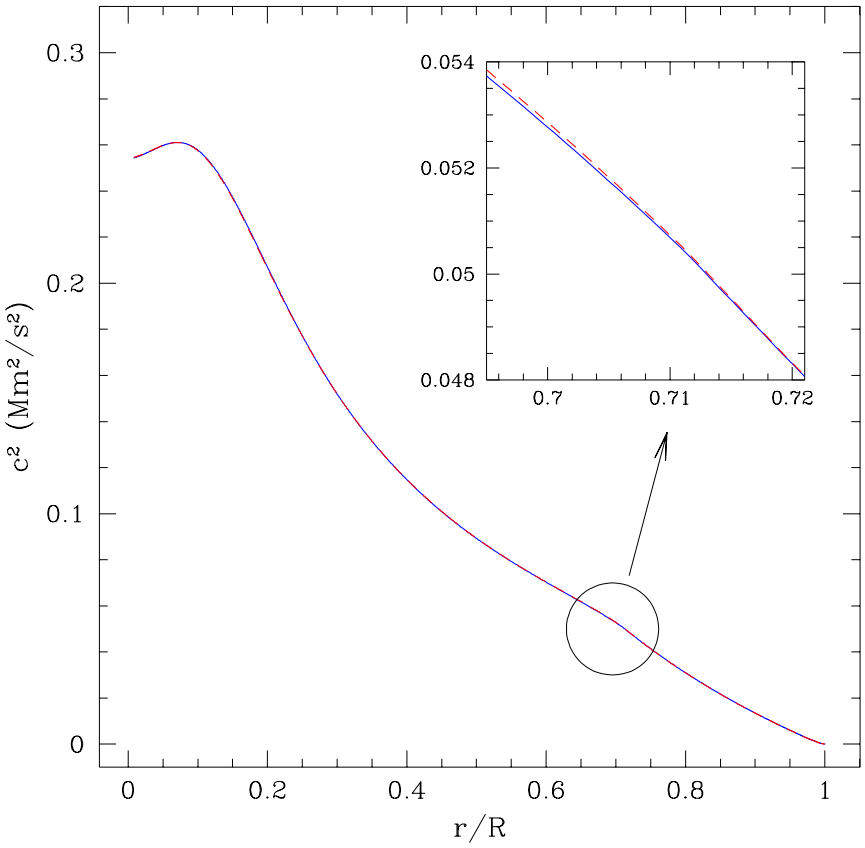

Figure 3: The dashed curve is the square of the spherically averaged sound speed in the Sun. The solid curve corresponds to a standard theoretical model. The magnitudes of the slopes of the curves are lower immediately beneath the convection zone, where the temperature gradient is too small to drive the instability. It is evident from the inset that the convectively unstable region of relatively high slope extends somewhat more deeply into the Sun than it does in the model.

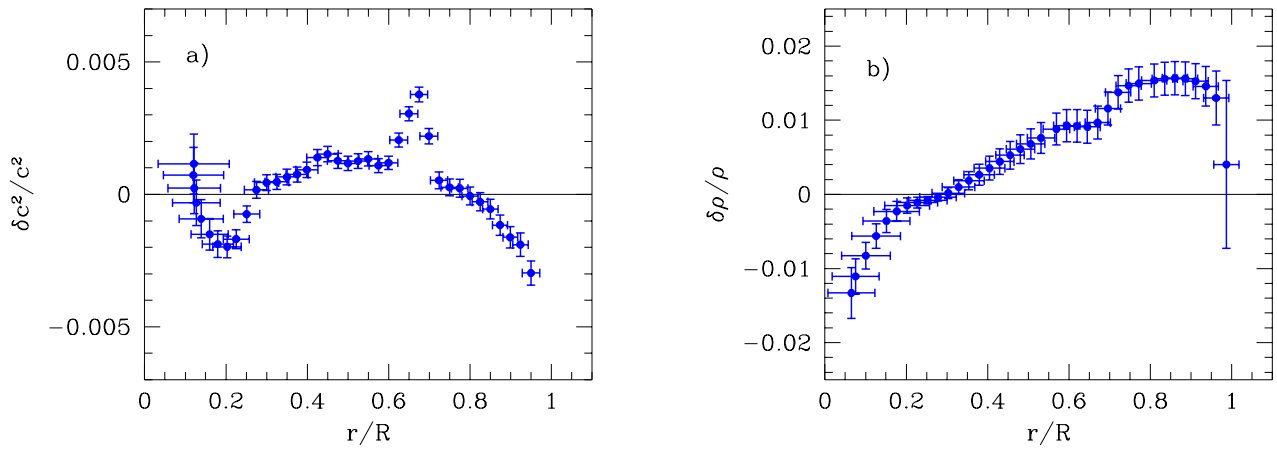

Figure 4: Relative differences $\delta u/u$ and $\delta\rho/\rho$ between $u = p/\rho$ and the density in the Sun and the standard model with gravitational settling of helium and heavy elements (3).

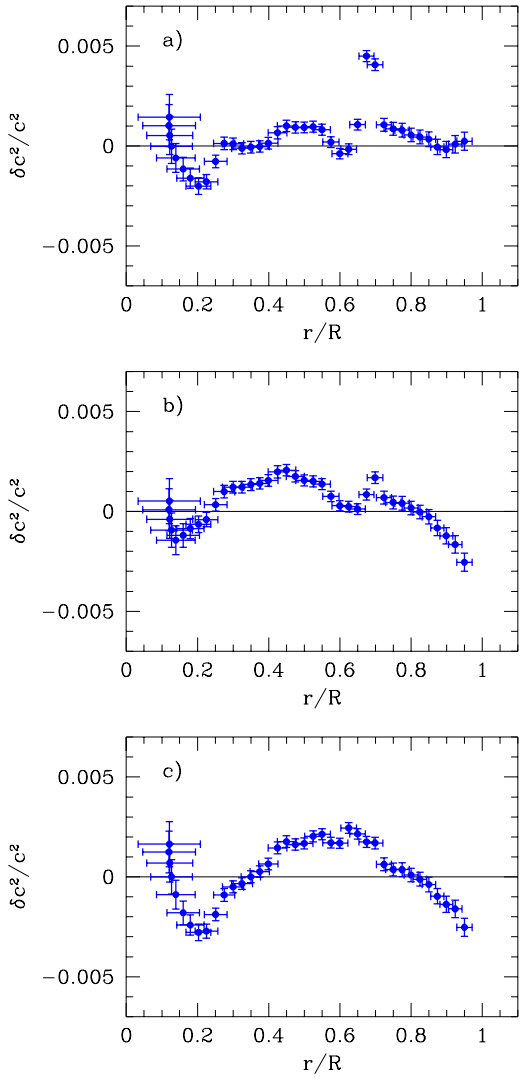

Figure 5: Relative differences $\delta u/u$ between u in the Sun and in various theoretical models. The theoretical models are A a model with weak mixing *(15)*, presumed to be generated by rotationally induced turbulence; B a similarly mixed model *(16)*; C a model with mass loss *(17)*; In order to produce a homogeneous comparison, the inversions are of the frequency differences: $\nu_\odot - \nu_s - (\nu_m - \nu_0)$, where $\nu_\odot$ are solar frequencies, ν_s are the frequencies of the standard solar model used in Fig. 4, and ν_m and ν_0 are frequencies computed with the same computer code with and without mixing (or mass loss) respectively. Thus they represent the effect incorporating mixing (or mass loss) into the reference model used in Fig. 4.

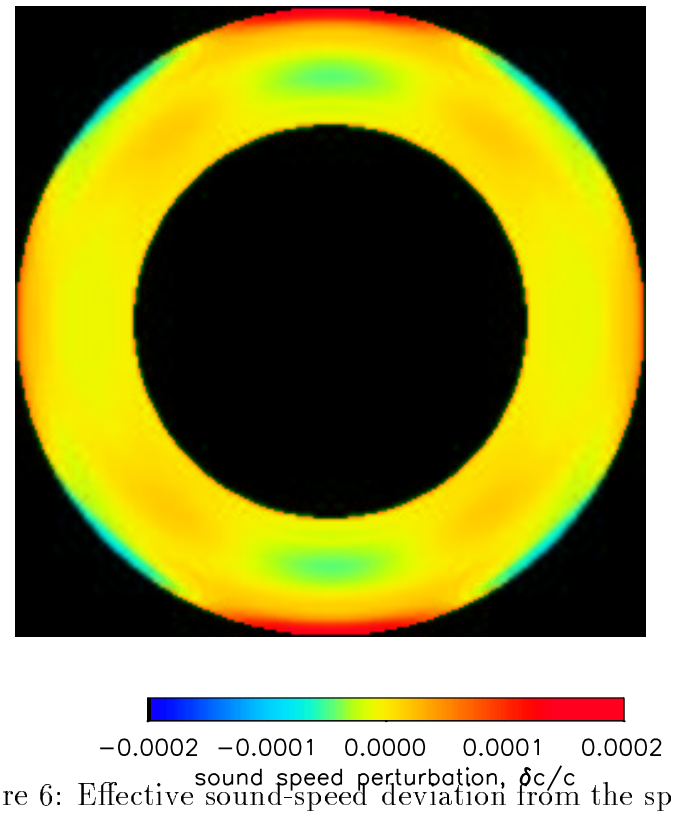

Figure 6: Effective sound-speed deviation from the spherical average.

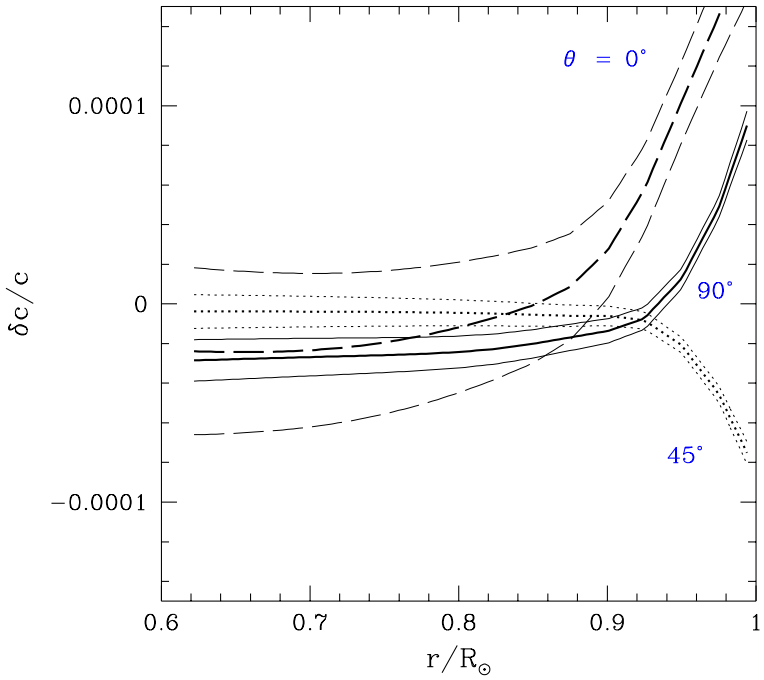

Figure 7: Relative sound-speed deviation from the spherical average, plotted against radius, at the equator (continuous curve), latitude 45^o (dotted) and the poles (dashed).